PVDF type AE Sensor monitoring system for AL-7075 surface polishing using fiber laser

Hyojeong Kim[a], Seounghwan Lee*[a], Juheon Lee [b], Sinyeop Lee [b],
Hyungjin Park [c], Jaehyeon Nam[c], Heehwan Lee [d]
[a]Dept. of Mechanical Engineering, BK21 FOUR ERICA-ACE center, Hanyang Univ., Republic of Korea; [b]HYU-KITECH joint Dept., Hanyang Univ., Republic of Korea; [c]Dept. of Mechanical Engineering, Hanyang Univ. ERICA, Republic of Korea; [d]Dept. of Mechanical Design Engineering, Hanyang Univ., Republic of Korea

ABSTRACT

Selective laser melting (SLM) is a combined process of melting and stacking three-dimensional products by fusing micro-metal powder using a laser. It has the advantage of manufacturing parts with complex structures with reduced production time. However, in the case of aluminum, the disadvantages of poor laser formability due to its high thermal conductivity, diffusivity, and reflectivity result in process defects such as bowling, pore, and poor surface quality. This study aims to develop a surface defect removal methodology during aluminum melting by laser processing and to enhance process automation capabilities by introducing a sensor monitoring scheme. In the laser experiments, aluminum specimens (AL-7075) with mechanical scratches were used and the level of surface defect removal during processing was classified depending on surface conditions. In addition, a PVDF-type acoustic emission (AE) sensor monitoring system was implemented to collect characteristic signals during the laser polishing of the machined surface(scratch). It was shown that the degree of surface defects removal and surface state could be effectively classified through a convolution neural network (CNN) utilizing the collected signals as input vectors.

Keywords: Laser post-processing, convolution neural network, surface defect, pvdf-type acoustic emission sensor

1. INTRODUCTION

Rapid prototyping, which can speed up repetitive design processes, is widely used in automobiles, transportation, aerospace, and defense industries to improve prototyping and product quality[1-3]. Among them, selective laser melting (SLM), a representative metal-based additive manufacturing technology, is a technology that uses a laser to melt the fine metal powder and pile them up one by one. It can process materials by finely adjusting the energy using a laser and manufacturing products with complex shapes, such as porous structures and lattice structures that cannot be manufactured with conventional material removal methods. Therefore, many studies using various metals have been conducted to manufacture mechanical parts in industries such as weapons, aviation, and space using SLM[4-6]. Gebhardt et al. manufactured tooth crowns and bridges designed by scanning actual teeth through SLM processes using materials such as tool steel, titanium, aluminum, stainless steel, nickel, cobalt chromium, and Inconel[7]. Jung et al. studied the properties of BMG according to crystal structure by manufacturing Fe-Co-based bulk metal glass (BMG, Bulk Metal Glass) with SLM[8]. Pehlivan et al. used SLM technology to produce porous structural artificial bones and joints made of titanium alloy[9], and Shapiro et al. succeeded in manufacturing composite antenna support using aluminum alloy material using SLM technology[10].

Especially aluminum is a highly specific strength, corrosion-resistant, and lightweight material that is widely used in various industries such as aviation, automobiles, weapons, and mechanical components[11-13.] To improve performance according to the requirements, aluminum parts production methods using SLM technology are continuously being researched. Bartkowiak et al. studied the behavior of alloys based on AL-Si powder alloys to make high-strength aluminum alloys through the SLM process. They developed a new lightweight material powder system according to the powder percentage and particle size[14].

*sunglee@hanyang.ac.kr; phone 82+ 31 400-4706; iml.hanyang.ac.kr

Laser-based Micro- and Nanoprocessing XVII, edited by Rainer Kling, Akira Watanabe, Wilhelm Pfleging,
Proc. of SPIE Vol. 12409, 124091C · © 2023 SPIE · 0277-786X
doi: 10.1117/12.2665278

They developed a new lightweight material powder system according to the powder percentage and particle size[14]. Louis et al. investigated and analyzed the oxidation effects of the component density by controlling the laser energy output to produce high-density aluminum parts with the SLM process[15]. Defects produced during SLM processing of aluminum and aluminum alloys can be found to be like those of conventional casting methods. Zhang et al. showed the types of aluminum alloys suitable for the SLM process and their microstructure. They studied balling, porosity, oxidation, residual stress, and cracks that may occur due to metal defects[16]. High-strength aluminum is lighter and stronger than steel and is used as a space and aviation material. Still, it has high thermal conductivity, thermal diffusivity, and reflectivity, resulting in surface defects such as bowling, pore, and poor surface quality during laser molding[17].

In this study, laser defect removal experiments were conducted with pre-machined (scratched) surfaces of aluminum (AL-7075). The level of surface defect removal during processing was examined for various process conditions. In addition, a PVDF-type acoustic emission (AE) sensor monitoring system was implemented to collect characteristic signals during the laser polishing. The degree of removal of each surface defect was classified through signal analysis using an AI technique (CNN).

2. EXPERIMENTAL SETUP

2.1 PVDF- type acoustic emission sensor

Acoustic emission (AE) is a phenomenon in which elastic waves are generated by releasing accumulated internal energy when a material is finely destroyed. AE can detect small dynamic changes such as plastic deformation of materials because it has a wide frequency range and high sensitivity for ultrasonic signals. Still, it requires professionals and expensive equipment for inspection, which is not economical. To overcome this advantage, acoustic emission monitoring was performed using the piezoelectric effect of PVDF. PVDF has the advantages of thermal stability and flexibility, excellent piezoelectricity, and low cost compared to AE sensors[18-20]. It also has a lower stiffness and electrical impedance than the AE sensor's main material, piezo ceramic, and is thinner[21]. Using acoustic emission transducers using piezoelectric films, Ciampa et al. tracked the location of the signal and identified its source[22]. De Rosa et al. studied structural condition monitoring using PVDF sensors as AE sensors and showed that damage, growth, and development of glass/epoxy laminates could be monitored using PVDF sensors[23]. Feng et al. manufactured AE sensors using PVDF instead of PZT[24]. The manufactured AE sensors have a superior signal-to-noise ratio (SNR) compared to commercial AE sensors and have shown approximately 13 times better performance in steel ball drop experiments. Bar et al. used a PVDF sensor to monitor the acoustic emission signals generated during static tensile loads of glass fiber-reinforced plastic composites. This confirms that the PVDF sensor is effective as an AE sensor[25]. Bordatcheve et al. showed that the frequency difference in the laser process occurs between 20 kHz and 180 kHz in monitoring the laser material removal process using copper brass plates[26]. Gu et al. analyzed that the welding AE signal of aluminum CO2 laser occurs between 6-17 kHz[27]. Duley et al. collected AE signals for carbon steel laser welding and showed that the AE signal changed depending on the laser output at 3-10 kHz[28]. The reason was indicated to be due to the combustion of the surface oxide. Previous papers show that AE signals from the laser process can be collected at frequencies between 1~100 kHz.

Therefore, in this study, the signals of the fiber laser process are collected using a PVDF sensor with a sensitivity of 1 to 100 kHz instead of the AE sensor.

2.2 Experimental setup

We used high-strength aluminum AL-7075, and Table 1 shows the workpiece components. Scratches on the surface were made by QM450A from Qmesys, with a tip that has a diameter of 30 μm, a speed of 1 mm/s, and a force of 100 mN. Figure 1 shows a schematic diagram of the devices used in the study.

Table 1. Compositions and mechanical properties of AL-7075[29].

Element (Wt.%)	Zn	Cu	Mg	Al
	5.1-6.1	1.2-2.0	2.1-2.9	89-91.6
Property	Tensile strength	Yield strength	Elastic modulus	Hardness (Brinell)
	570 Mpa	455 Mpa	72 Gpa	150 HB

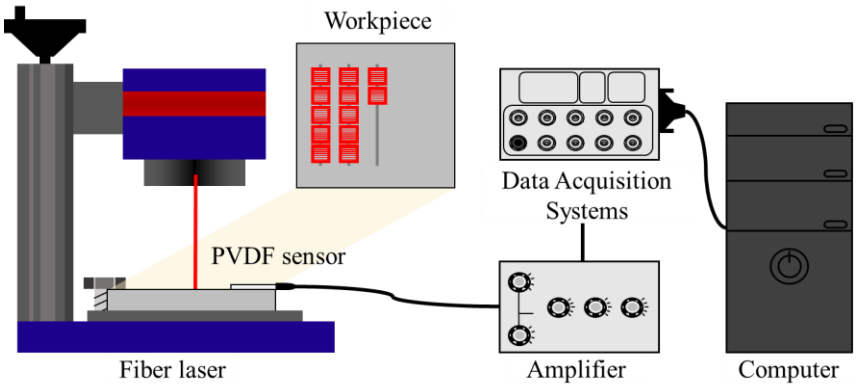

Figure 1. Schematic diagram of experimental setup.

The fiber laser used YF200S, a fiber laser marker manufactured by YOOSUNGENG, as the heat source used in this experiment, has a wavelength of 1064 nm, a beam diameter of 80μm, and a maximum power of 20W. Table 2. shows the experimental conditions of the laser, which were determined through preliminary experiments.

Table 2. Experimental conditions of the laser processing.

Laser Frequency (kHz)	Scan speed (mm/s)	Energy (%)	Line gap (mm)
20	3	18, 38, 58	0.03

We monitored laser polishing under three different laser energy output conditions. The three conditions of insufficient, sufficient, and excess were processed to different energy output conditions of 18, 38, and 58%. The PVDF-type AE sensor was attached to the surface of the specimen using grease. The attached PVDF is SDT1-028k, which has the advantage of preventing background noise. During the laser process, the AE signal generated from the specimen was converted from mechanical energy to electrical energy by the PVDF-type AE sensor. For AE signals, 2000 signals were collected for each experimental condition using NI's LabVIEW. Table 3 shows the signal collection conditions for the PVDF sensor.

Table 3. PVDF-type AE sensor acquisition setup.

Low Frequency (kHz)	High Frequency (kHz)	Gain (dB)	Sampling rate (kHz)
1	100	20	200

After processing, we used Nikon's Eclipse LV100 optical microscope to compare the surface conditions and check defects before and after processing. The tendency was confirmed by using the degree of removal of defects or scratches on each surface as an indicator of the degree of machining. In addition, we measured the surface roughness using a stylus (SJ-410 form Mitutoyo) to check the precision level and processing condition before and after processing.

3. EXPERIMENTAL RESULTS

3.1 AE signal and Surface roughness

Surface roughness should be measured because even a slight change in the process has a sensitive effect and significantly impacts surface precision. According to the three laser energy output conditions, surface roughness was measured for the processed surface. Figure 2, Table 4 shows the roughness of the surface before and after laser polishing and the roughness of the surface produced by the scratch tester. The typical surface roughness of an AL-7075 specimen is 1.6 μm, and minor scratches on the surface increase the surface roughness by 0.2 μm. In addition, removing scratches through laser polishing has a surface roughness of 1.175 μm, 0.857 μm, and 6.274 μm depending on insufficient, sufficient, and excess. Excessive laser processing caused surface defects such as porosity, which increased surface roughness about four times compared to the typical surface roughness.

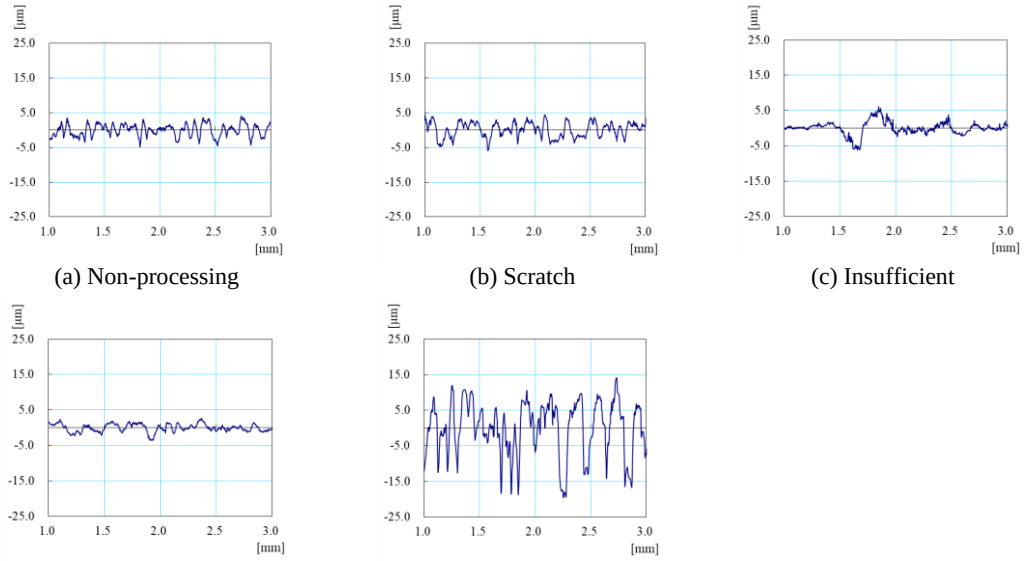

(a) Non-processing (b) Scratch (c) Insufficient

(d) Sufficient (e) Excess

Figure 2. Surface roughness shape before and after laser polishing.

Table 4. Surface roughness before and after laser polishing

Condition (Surface roughness, Ra)				
Non-processing	Scratch	Insufficient (Energy 18%)	Normal (Energy 38%)	Excess (Energy 58%)
1.599 μm	1.878 μm	1.175 μm	0.857 μm	6.274 μm

The optical microscope image in Figure 3 shows the condition of the surface before and after processing. In the case of laser polishing with 18% of power energy, as illustrated in Fig. 3. (a), scratches were not removed and processed with sufficient energy, so it was judged to be insufficient. Laser polishing with 38% energy was classified as sufficient because all scratches on the surface were removed and processed with sufficient energy, as shown in Figure 3(b). In the case of laser polishing with 58% energy, the laser-processed surface in Figure 3(c) was considered blackened, so excessive energy was used and classified as excess.

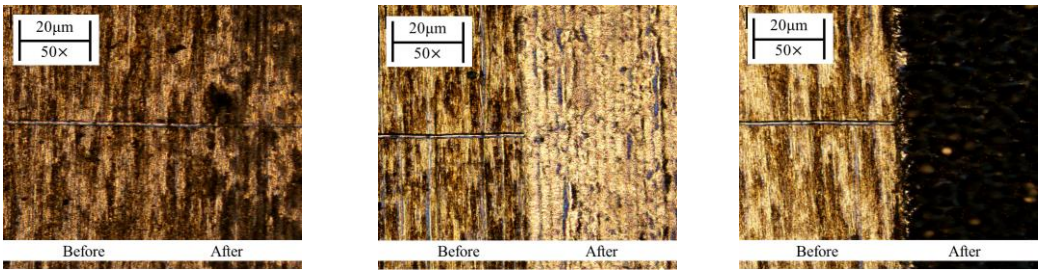

(a) Insufficient (b) Sufficient (c) Excess

Figure 3. Surface condition of AL-7075 before and after laser polishing.

Optical microscope images and surface roughness results show significant differences depending on the energy percentage of the laser, which can be correlated with AE signals under different conditions. The sampling rate in the experiments in this study is 200 kHz, which has a high sampling rate that also increases the number of data generated. In this experiment, 200,000 data per signal, a total of 6000 signals were generated. Figure 4 shows the AE source signal generated for each laser condition. A large amount of data makes it difficult to classify the features of each signal or find any differences. Therefore, Fast Fourier Transform (FFT), a frequency analysis company, was used to see the

characteristics of each signal. The FFT converts complex signals into frequency domains, as shown in Figure 4, to analyze the signals for each frequency range. Figure 5 shows the FFT image of the signal in Figure 4. These graphs allow us to find the characteristics of each signal's frequency band that were not identified in the raw signal graph in Figure 4. Figure 5(a) shows the processed signal by setting the laser output energy to 18% and shows that the frequency decibel is lower than other laser output process signals. Significantly, 40-50 kHz and 80-90 kHz are the frequency ranges where decibel changes are most noticeable. Compared to Fig.5(a), Fig. 5(b) shows larger decibels at the frequency range. Fig. 5(c) is the highest laser output process signal graph, showing higher decibels overall compared to Fig. 5(a) and (b).

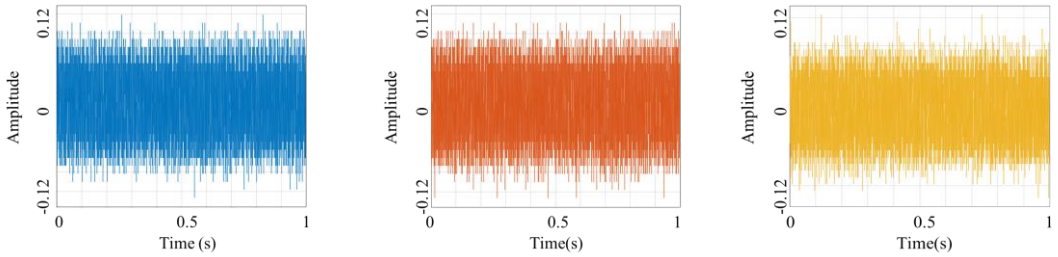

(a) Insufficient (b) Sufficient (c) Excess

Figure 4. Laser polishing raw signal from PVDF type AE sensor.

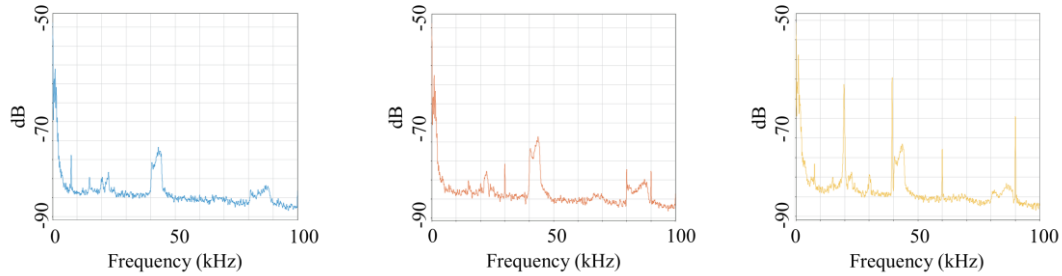

(a) Insufficient (b) Sufficient (c) Excess

Figure 5. FFT result of laser polishing raw signal from PVDF type AE Sensor.

The frequency difference according to laser output can be seen in Fig 6. This shows that the difference in the characteristics of the signal for each frequency band is based on the laser output energy and the removal signal of the scratch.

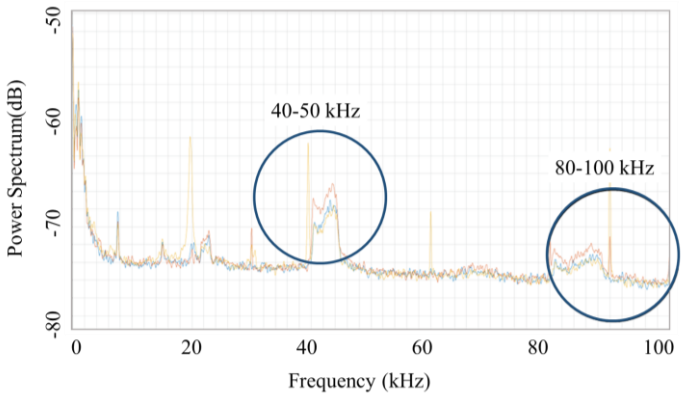

Figure 6. Comparison of FFT result of laser polishing signals.

3.2 Convolution neural network

In this experiment, we used the most appropriate convolutional neural network (CNN) algorithm to classify the imaged data to analyze the differences in signal features, as shown in Figure 6. The CNN algorithm is one of the main algorithms used to learn pictures and images, and it extracts patterns and characteristics of images and learns and classifies them by itself[30]. In addition, CNN introduced convolutional operations to solve the overfitting problem. With CNN, we can find patterns in numerous images collected and extract attributes to reduce the time required for classification[31].

In this experiment, FFT images were used as image data for CNN. In the case of acoustic emission data, the preprocessing process is essential due to a large amount of data, and FFT produced a total of 6,000 images in units of 200,000. Therefore, for CNN training speed, the image size was adjusted to 227x227, and the image was grayscaled to simplify the algorithm. Figure 7 shows the reconstructed FFT image for use as image data for CNN. The structure and description of the CNN network model can be found in Table 5.

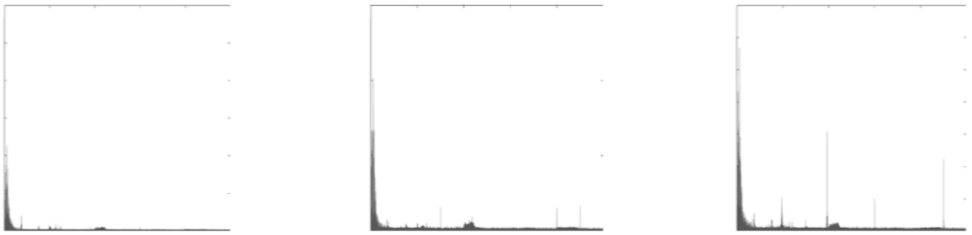

(a) Insufficient (b) Sufficient (c) Excess

Figure 7. FFT grayscale conversion image of laser polishing signal from PVDF type AE Sensor.

Table 5. Structure of CNN network model for classification.

No.	Layer name	Description
1	Imageinput	227x227x3 images with “zero center” normalization
2	Convolution_1	32, 3x3x3 convolutions with stride [1 1] and padding ‘same’
3	Batchnorm_1	Batch normalization with 32 channels
4	Relu_1	Activation function of convolution layer
5	Maxpool_1	5x5 max pooling with stride [1 1] and padding ‘same’
6	Convolution_2	32, 3x3x32 convolutions with stride [1 1] and padding 'same'
7	Batchnorm_2	Batch normalization with 32 channels
8	Relu_2	Activation function of convolution layer
9	Maxpool_2	5x5 max pooling with stride [1 1] and padding ‘same’
10	Convolution_3	32, 3x3x32 convolutions with stride [1 1] and padding 'same'
11	Batchnorm_3	Batch normalization with 32 channels
12	Relu_3	Activation function of convolution layer
13	Maxpool_3	5x5 max pooling with stride [1 1] and padding ‘same’
14	Fully connected	3 fully connected layer
15	Softmax	Activation function of convolution layer
16	Classoutput	Classoutput

The total data used for CNN was 6,000, and 2000 signals were collected for each type, and 70% were cross-validated with the verification data of 30% of the training data. The CNN in this experiment used three hidden layers, and overfitting was prevented through the batchnormal layer. R-type and Softmax functions were used as activation functions. The training cycle information is Epoch 28/30, Iteration 1221, Iteration per epoch 45, and Maximum Iteration 1350. Frequency 10 Iteration as a verification method, and the learning rate is 0.005. As a result, 99.5% training accuracy and 99.226% verification accuracy were achieved using Adam Optimizer (Figure 8).

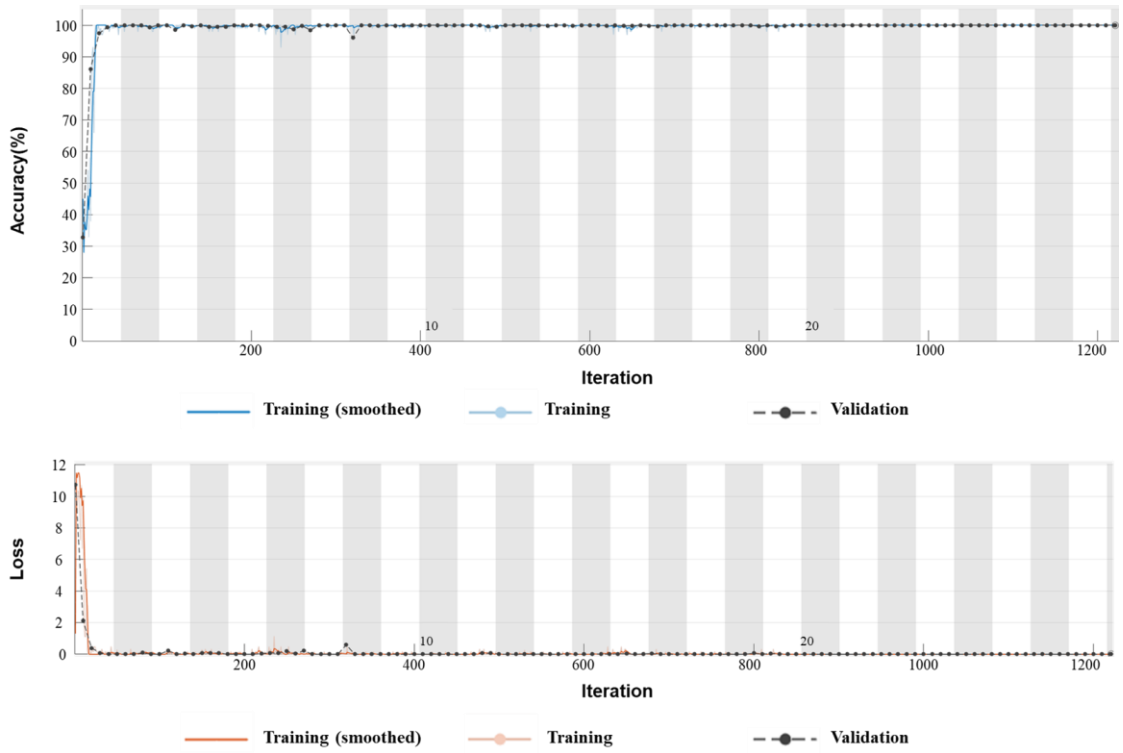

Figure 8. CNN training performance.

4. CONCLUSIONS

PVDF-type AE sensor monitoring was proposed to classify the degrees of surface defect removal during laser polishing of aluminum specimens, which is directly applicable to the SLM process. Conclusions are as follows:

- By comparing optical microscope images and surface roughness vales to AE signals during laser polishing, strong correlations were observed between AE signals and surface characteristics.
- The degree of scratch removal and surface condition was classified into three types: insufficient, sufficient, and excessive, and the frequency bands showing significant signal characteristics were observed as 40-50 and 90-100 kHz.
- With the FFT images generated from the AE signals during laser polishing as inputs, proposed CNNs produces reliable outcomes - the classification accuracy of 99.226%.

It has been shown that the PVDF-type sensor can detect meaningful AE signals during the laser polishing process and identify surface characteristics according to the laser output energy. For this reason, PVDF-type AE Sensors can be a viable alternative for conventional AE sensors for laser processing signal acquisition.

REFERENCES

[1] Upcraft, S., & Fletcher, R., "The rapid prototyping technologies," Assembly Automation (2003).

[2] Song, Y., Yan, Y., Zhang, R., Xu, D., & Wang, F., "Manufacture of the die of an automobile deck part based on rapid prototyping and rapid tooling technology," Journal of materials processing technology, 120(1-3), 237-242 (2002).

[3] Thomas, C. L., Gaffney, T. M., Kaza, S., & Lee, C. H., "Rapid prototyping of large scale aerospace structures," In 1996 IEEE Aerospace Applications Conference, Proc. IEEE, 4, 219-230 (1996).

[4] Brandt, M., Sun, S. J., Leary, M., Feih, S., Elambasseril, J., & Liu, Q. C., "High-value SLM aerospace components: from design to manufacture," In Advanced Materials Research Trans Tech Publications Ltd., 633, 135-147 (2013).

[5] Ferro, C. G., Varetti, S., De Pasquale, G., & Maggiore, P., "Lattice structured impact absorber with embedded anti-icing system for aircraft wings fabricated with additive SLM process," Materials Today Communications, 15, 185-189 (2018).

[6] Stolt, R., & Elgh, F., "Introducing design for selective laser melting in aerospace industry." Journal of Computational Design and Engineering, 7(4), 489-497 (2020).

[7] Gebhardt, A., Schmidt, F. M., Hötter, J. S., Sokalla, W., & Sokalla, P., "Additive manufacturing by selective laser melting the realizer desktop machine and its application for the dental industry," Physics Procedia, 5, 543-549 (2010).

[8] Jung, H. Y., Choi, S. J., Prashanth, K. G., Stoica, M., Scudino, S., Yi, S., ... & Eckert, J., "Fabrication of Fe-based bulk metallic glass by selective laser melting: A parameter study," Materials & Design, 86, 703-708 (2015).

[9] Pehlivan, E., Džugan, J., Fojt, J., Sedláček, R., Rzepa, S., & Daniel, M., "Post-processing treatment impact on mechanical properties of SLM deposited Ti-6Al-4 V porous structure for biomedical application," Materials, 13(22), 5167 (2020).

[10] Shapiro, A. A., Borgonia, J. P., Chen, Q. N., Dillon, R. P., McEnerney, B., Polit-Casillas, R., & Soloway, L., "Additive manufacturing for aerospace flight applications," Journal of Spacecraft and Rockets, 952-959 (2016).

[11] Holt, R. T., Wallace, R., Wallace, W., & DuQuesnay, D. L., "RRA heat treatment of large Al 7075-T6 components," NATIONAL RESEARCH COUNCIL OF CANADA OTTAWA (ONTARIO) INST FOR AEROSPACE RESEARCH (2000).

[12] Was, G. S., & Pelloux, R. M., "The effect of shot peening on the fatigue behavior of alloy 7075-T6," Metallurgical Transactions A, 10(5), 656-658 (1979).

[13] Kelly, A., & Zweben, C. H., [Comprehensive composite materials], Elsevier, (2000).

[14] Bartkowiak, K., Ullrich, S., Frick, T., & Schmidt, M., "New developments of laser processing aluminium alloys via additive manufacturing technique," Physics procedia, 12, 393-401 (2011).

[15] Louvis, E., Fox, P., & Sutcliffe, C. J., "Selective laser melting of aluminium components," Journal of Materials Processing Technology, 211(2), 275-284 (2011).

[16] Zhang, J., Song, B., Wei, Q., Bourell, D., & Shi, Y., "A review of selective laser melting of aluminum alloys: Processing, microstructure, property and developing trends," Journal of Materials Science & Technology, 35(2), 270-284 (2019).

[17] Wang, Z., Ummethala, R., Singh, N., Tang, S., Suryanarayana, C., Eckert, J., & Prashanth, K. G., "Selective laser melting of aluminum and its alloys," Materials, 13(20), 4564 (2020).

[18] Murayama, N., Nakamura, K., Obara, H., & Segawa, M., "The strong piezoelectricity in polyvinylidene fluroide (PVDF)," Ultrasonics, 14(1), 15-24 (1976).

[19] Platte, M., "PVDF ultrasonic transducers for non-destructive testing," Ferroelectrics, 115(4), 229-246 (1991).

[20] Hurmila, S., Stubb, H., Pitkänen, J., Lahdenperä, K., Penttinen, A., Suorsa, V., & Tauriainen, A., "Ultrasonic transducers using PVDF," Ferroelectrics, 115(4), 267-278 (1991).

[21] Shirinov, A. V., & Schomburg, W. K., "Pressure sensor from a PVDF film," Sensors and Actuators A: Physical, 142(1), 48-55 (2008).

[22] Ciampa, F., & Meo, M., "Acoustic emission source localization and velocity determination of the fundamental mode A0 using wavelet analysis and a Newton-based optimization technique," Smart Materials and Structures, 19(4), 045027 (2010).

[23] De Rosa, I. M., & Sarasini, F., "Use of PVDF as acoustic emission sensor for in situ monitoring of mechanical behaviour of glass/epoxy laminates," Polymer Testing, 29(6), 749-758 (2010).

[24] Feng, G. H., Tsai, M. Y., & Jeng, Y. R., "A micromachined, high signal-to-noise ratio, acoustic emission sensor and its application to monitor dynamic wear," Sensors and Actuators A: Physical, 188, 56-65 (2012).
[25] Bar, H. N., Bhat, M. R., & Murthy, C. R. L., "Parametric analysis of acoustic emission signals for evaluating damage in composites using a PVDF film sensor," Journal of Nondestructive Evaluation, 24(4), 121-134 (2005).
[26] Bordatchev, E. V., & Nikumb, S. K., "Effect of focus position on informational properties of acoustic emission generated by laser–material interactions," Applied Surface Science, 253(3), 1122-1129 (2006).
[27] Gu, H., & Duley, W. W., "Acoustic emission and optimized CO2 laser welding of steel sheets," In International Congress on Applications of Lasers & Electro-Optics Laser, Institute of America, 1994(1), 77-85 (1994).
[28] Duley, W. W., & Mao, Y. L., "The effect of surface condition on acoustic emission during welding of aluminium with CO2 laser radiation," Journal of Physics D: Applied Physics, 27(7), 1379 (1994).
[29] Gale, W. F., & Totemeier, T. C. (Eds.)., [Smithells metals reference book], Elsevier, (2003).
[30] LeCun, Y., Bengio, Y., & Hinton, G., "Deep learning," nature, 521(7553), 436-444 (2015).
[31] Krizhevsky, A., Sutskever, I., & Hinton, G. E., "Imagenet classification with deep convolutional neural networks," Communications of the ACM, 60(6), 84-90 (2017).